Passivity-based control for a rolling-balancing system: The nonprehensile disk-on-disk.

Alejandro Donaire, *Member, IEEE,* Fabio Ruggiero, *Member, IEEE,* Luca Rosario Buonocore, Vincenzo Lippiello, *Member, IEEE,* Bruno Siciliano, *Fellow, IEEE*

***Abstract*—In this paper, we propose a passivity-based control design for a rolling-balancing system called the disk-on-disk. The stabilization of the desired equilibrium is obtained via energy shaping and damping injection. The disk-on-disk is an underactuated mechanical system composed of two disks arranged one on top of the other. The top disk, which we call the object, is free to roll without slipping on the lower disk, which we call the hand. The hand is actuated by a controlled torque, while the object is unactuated. The control objective is to balance the object at the upright position and drive the hand to a desired angle. We design an energy shaping controller without solving the partial differential equations, which rise from the matching equation. We assess the performance of the controller by both simulations and experiment results, which also verify the practical applicability of the design approach.**

***Index Terms*—Rolling-balancing systems, passivity-based control, nonprehensile systems, energy shaping.**

I. Introduction

MANIPULATING an object without grasping is a task known as *nonprehensile manipulation*. Although this class of manipulation problems has received great attention by the research community, it is still rather far from being fully solved for robotic applications [1], [2], [3]. There are several advantages in nonprehensile dynamic manipulation. Since the object is not caged between fingertips during the task, it is possible to manipulate the object outside the robot workspace by allowing both contact and non-contact interaction between the robot and the object, e.g. by throwing and catching the object [1]. Moreover, it is possible to control more object degrees of freedom than the actuators of the robotic platform [3], [4]. In several industrial applications it is not directly possible to manipulate the object through firm or fine/precise manipulation, therefore only nonprehensile manipulation is allowed to accomplish the task, e.g. using vibratory platforms [1]. Dynamic nonprehensile manipulation tasks are performed by surgeons with their instruments during operations, for example when they push away an organ or an artery. For this class of systems, the control design has to take into account the dynamics of both the robot and the object, which increases the complexity of the design. Thus, challenging problems in high-speed sensing and control fields arise in nonprehensile manipulation.

A classical approach for control design of dynamic nonprehensile tasks is to divide a complex action into simpler primitives and subtasks such as rolling, pushing, throwing, batting, and juggling, to mention some of them [1], [5], [6]. In this paper, we concentrate on a particular primitive of nonprehensile manipulations, that is *rolling*, considering the disk-on-disk (DoD) system. We address the stabilization-balancing problem of the DoD using passivity-based control and port-Hamiltonian (pH) systems (see [7] and [8] for a survey on these topics). The DoD controller proposed in this paper is designed under the assumption the disks are in contact. Such assumption cannot be ensured in the physical set-up since the disks are no mechanically attached. However, the experiments show that the controller performs satisfactory well. Similar considerations have been used in [5], [6], [9].

Among other examples of nonprehensile rolling primitives we can mention the ball and plate (B&P), the ball and beam (B&B) and the "butterfly" system. The B&P is a nonholonomic system for which it has been shown that there exist an admissible path between any two configurations [10]. A PID-based control was proposed in [11] to stabilize the linearized model and a sliding mode controller is instead employed in [12]. The B&P problem is also related to the field of spherical robots [13]. Two planning methods for this class of systems are presented in [14], which are based on minimum energy and time approaches. The B&B system considers the problem of stabilizing the position of a ball along a beam. Since B&B system is not full-feedback linearizable, an approximated partial feedback linearization (PFL) and output feedback controller were proposed in [15] and [16] respectively. Alternatively, an interconnection and damping assignment passivity-based control (IDA-PBC) design is proposed in [17], a backstepping controller is designed in [18], and a sliding control law is instead proposed in [19]. Nonprehensile rolling systems where the ball's (or disk's) center of mass does not coincide with its geometric center are more challenging (see for example [20]). The control of a dynamically balanced asymmetrical sphere with three internal rotors is described in [21]. Finally, the so-called

A. Donaire, F. Ruggiero, L.R. Buonocore, V. Lippiello and B. Siciliano are with CREATE Consortium and PRISMA Lab, Department of Electrical Engineering and Information Technology, University of Naples Federico II, Via Claudio 21, 80125, Naples, Italy. Email: {alejandro.donaire, fabio.ruggiero, lucarosario.buonocore, vincenzo.lippiello, bruno.siciliano}@unina.it.

A. Donaire is also with the School of Engineering, The University of Newcastle, Australia.

"butterfly" juggling action, in which planar rolling is involved, has been investigated in [4], [6], [22]. A controller for a ball rolling in an asymmetrical bowl that can be accelerated along one linear direction is proposed in [23]. Planning and control problems of a ball rolling on curved surfaces are also investigated in [24], [25].

In particular, in this paper we consider the rolling between two circular surfaces as the primitive. The case study is the balancing of a disk that is free to roll on an actuated disk. We refer to the former disk as the object, and the latter as the hand. This system, introduced in [9], can be considered as an example for nonprehensile rolling primitive. The theoretical and technological novelties introduced by this paper are as follows:

- In [5] and [9] the DoD controller is designed using feedback linearization and backstepping, respectively. The backstepping design considers only the stabilization of the object at the upright position, leaving the hand uncontrolled. The feedback linearization controller stabilizes the positions of both the object and the hand. In this paper, we propose to shift the control design to the passivity approach to stabilize both the object and the hand to the desired equilibrium. An important feature of this approach is that the control design exploits the energy and interconnection properties of the physical system without the need of nonlinear cancellations, which in general compromise the robustness of the closed loop. This approach differs from the standard feedback linearization where a linear dynamics is imposed at the expense of cancelling all the nonlinear dynamics of the system.
- The passivity-based controller is developed via energy shaping and damping injection [17]. We follow the approach in [26], where the energy is shaped without the need of solving partial differential equations (PDEs). In [26] the requirement of energy shaping that the closed loop should preserve the form of a mechanical system is dropped. However, we show that the controller proposed here satisfies the so-called *matching equation* [17]. Therefore, the controller belongs to the class of IDA-PBC controllers, and the closed loop can be written in the pH form. The control design here is simpler since there is no need of solving PDEs.
- In this work we develop a less demanding hardware with respect to [5], [9]. Indeed, the camera and control frame-rate is downgraded from 800 to 75 Hz. In addition, the disks are vertically aligned, and thus the full-gravity field is considered. The experimental results show that the proposed controller design has a good performance on this less demanding set-up.
- In the experiments, we do not consider the addition of integral action to robustify the controller as done in [5]. However, the proposed passivity-based controller performs satisfactorily well and cope with uncertainties without the need of an integral action redesign.

The outline of the paper is as follows. The pH framework is briefly revised in Section II. The dynamic model of the DoD system and the control design are discussed in Section III. Section IV presents simulations of the control system, whilst the experiment results are shown in Section V. Final discussions are provided in Section VI.

II. Port-Hamiltonian framework

The dynamics of a general class of mechanical systems can be described as a pH system as follows

$$\begin{bmatrix} \dot{q} \\ \dot{p} \end{bmatrix} = \begin{bmatrix} 0 & I_n \\ -I_n & 0 \end{bmatrix} \nabla H(q,p) + \begin{bmatrix} 0 \\ G(q) \end{bmatrix} \tau, \qquad (1)$$

where $q \in \mathbb{R}^n$ are the generalized coordinates, $p \in \mathbb{R}^n$ are the generalized momenta defined as $p = M\dot{q}$, $\tau \in \mathbb{R}^m$ are the generalized input forces, $G : \mathbb{R}^n \to \mathbb{R}^{n\times m}$ is the input matrix, and I_n is the $n-$dimensional identity matrix. The function $H : \mathbb{R}^{n\times n} \to \mathbb{R}$, which represents the total energy of the system, is the Hamiltonian given by

$$H(q,p) = \frac{1}{2} p^\top M^{-1}(q) p + V(q), \qquad (2)$$

where $M : \mathbb{R}^n \to \mathbb{R}^{n\times n}$ is the mass matrix and $V : \mathbb{R}^n \to \mathbb{R}$ is the potential energy.

A feature of pH systems is that they are cyclo-passive with input τ and output $y = G^\top(q)M^{-1}p$, and storage function $H(q,p)$. Moreover, if $H(q,p)$ is bounded from below, then the pH system is passive [8].

The stabilization problem of the mechanical system (1) using IDA-PBC is to find a control law $\tau = \bar{\tau}(q,p)$ such that the closed loop has a stable equilibrium at the desired point $(q,p) = (q_\star, 0)$, with Lyapunov function

$$H_d(q,p) = \frac{1}{2} p^\top M_d^{-1}(q) p + V_d(q), \qquad (3)$$

with $M_d > 0$, and $q_\star = \arg\min V_d(q)$, and this minimum is isolated. The matrix $M_d : \mathbb{R}^n \to \mathbb{R}^{n\times n}$ and the function $V_d : \mathbb{R}^n \to \mathbb{R}$ are, respectively, the desired mass matrix and desired potential energy to be chosen. It is also required that the closed-loop dynamics retain the pH form

$$\begin{bmatrix} \dot{q} \\ \dot{p} \end{bmatrix} = \begin{bmatrix} 0 & M^{-1}M_d \\ -M_dM^{-1} & J_2(q,p) - R(q,p) \end{bmatrix} \nabla H_d(q,p), \quad (4)$$

where J_2 is a skew-symmetric matrix to be chosen, and $R = R^\top \geq 0$ is the damping injection matrix [17].

In the most general case, the control design using IDA-PBC for mechanical systems involve the task of solving a set of PDEs (see e.g. [17]). Indeed, the control law rendering the system (1) in the closed-loop dynamics of the form (4) should satisfy the so-called *matching equation*

$$-\nabla_q H + G\tau = -M_d\, M^{-1}\, \nabla_q H_d + (J_2 - R)\, M_d^{-1}\, p. \quad (5)$$

However, there exist constructive results to overcome the difficulty of solving the PDEs [26], [27].

III. Rolling manipulation.

The DoD balancing system is an example of a primitive for nonprehensile manipulation. The system is shown in Fig. 1. The bottom disk represents the manipulator, and the disk on top is the object to be balanced in the upright position. For the purpose of control design, we make the following assumptions:

- The hand rotates about its centre P_h, whilst there is no translational motion.
- The object is always in point contact with the hand.
- The object rolls on the hand without slipping.

Notice that these assumptions imply that the object cannot depart from the hand. Only from the control design perspective, the problem thus becomes a prehensile manipulation problem. However, the real system does not necessary satisfy these assumptions and it is intrinsically a nonprehensile system. As it will be shown in the experiments, the controller performs satisfactory even if the assumptions are not a priori ensured at all time.

The dynamic model of the DoD, under the assumptions above, has been derived in [9] using the coordinates (θ, s), where θ is the angle of the hand and s is the length of the arc from the q-axis to the contact point, with the positive convention taken on the counterclockwise direction (see Figure 1). A detailed formulation of the DOD model in these coordinates can be found in [9].

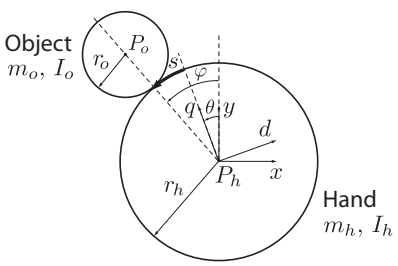

Fig. 1. Idealised physical scheme of the disk-on-disk system.

A. Disk-on-Disk model

A model, more convenient for our control design, is obtained by expressing the DoD dynamics given in [9] in coordinates (θ, φ), where φ is the deviation angle of the object from the upright position. The deviation angle is related with θ and s as follow

$$\varphi = \theta + \frac{s}{r_h}. \tag{6}$$

Using this change of coordinates, the dynamics of the DoD can be equivalently written in the pH form by defining[1] $q = \text{col}(\theta, \varphi)$ and momenta $\mathfrak{p} = \text{col}(\mathfrak{p}_1, \mathfrak{p}_2) = \mathcal{M}\dot{q}$, with

$$\mathcal{M} = \begin{bmatrix} M_{11} & M_{12} \\ M_{21} & M_{22} \end{bmatrix}, \tag{7}$$

[1]In this paper, a column vector $v \in \mathbb{R}^n$ with entries a_i with $i = 1, \cdots, n$ is noted as $v = \text{col}(a_1, \cdots, a_n)$.

where $M_{11} = (m_o + m_h)r_h^2$, $M_{12} = M_{21} = -m_o r_h(r_o + r_h)$, $M_{22} = 2m_o(r_h + r_o)^2$, and potential energy function

$$V(\varphi) = c_g \cos(\varphi), \tag{8}$$

where $c_g = m_o g(r_h + r_o)$, g is the gravity constant, I_h and r_h are the moment of inertia and the radius of the hand, respectively. The moment of inertia, radius and mass of the object are noted as I_o, r_o and m_o, respectively.

The dynamics in pH form is as follows

$$\begin{bmatrix} \dot{q} \\ \dot{\mathfrak{p}} \end{bmatrix} = \begin{bmatrix} 0 & I_n \\ -I_n & 0 \end{bmatrix} \nabla \mathcal{H}(q, \mathfrak{p}) + \begin{bmatrix} 0 \\ \mathcal{G} \end{bmatrix} \tau_h, \tag{9}$$

with $\mathcal{G} = \text{col}(1, 0)$ and Hamiltonian

$$\mathcal{H}(q, \mathfrak{p}) = \frac{1}{2}\mathfrak{p}^\top \mathcal{M}^{-1}\mathfrak{p} + V(\varphi). \tag{10}$$

Contact forces. The DoD model (9) relies on the assumptions that the object and the hand are always in contact and there is not slipping. As discussed in [28, Chap. 5], by using a simple *Coulomb model* for frictional forces (see [29] for more elaborated models), the conditions on the normal and frictional forces that ensure rolling can be written as

$$f_n > 0, \tag{11}$$

$$|f_f| \leq \mu f_n, \tag{12}$$

where f_n and f_f are the normal and frictional forces, respectively, and $\mu > 0$ is the frictional coefficient. Further, the normal and frictional forces can be written as follows

$$f_n = m_o(\ddot{y}_o + g)\cos(\varphi) - m_o \ddot{x}_o \sin(\varphi), \tag{13}$$

$$f_f = m_o(\ddot{y}_o + g)\sin(\varphi) + m_o \ddot{x}_o \cos(\varphi), \tag{14}$$

where x_o and y_o are the components of the center of the object P_o. Using the DoD dynamics, the expression (13) and (14) can be also written as follows

$$f_n = m_o g \cos(\varphi) - m_o(r_h + r_o)\dot{\varphi}^2, \tag{15}$$

$$f_f = \frac{m_o(r_h + r_o)}{M_{11}M_{22} - M_{12}^2}\Big[M_{12}\tau_h - M_{11} c_g \sin(\varphi)\Big] + m_o g \sin(\varphi). \tag{16}$$

The control design in this paper, as in [5], does not consider explicitly the constraints (11) and (12). However, we will show later that the model assumptions are satisfied by computing the normal and frictional forces using data from experiments and verifying that the constraints are met.

B. Control objective

We aim at designing an IDA-PBC controller to stabilize the DoD system at the equilibrium given by $q_\star = \text{col}(\theta_\star, \varphi_\star)$ and $\mathfrak{p}_\star = \text{col}(0, 0)$. There are two classes of equilibrium points of interest. The first class corresponds to the equilibria where the final position of the hand is not of interest, that is $q_{\star 1} = \text{col}(\bar{\theta}, 0)$ with $\bar{\theta}$ any constant angle of the hand. The second class of equilibria corresponds to the case where the final position of the hand is specified $q_{\star 2} = \text{col}(\theta_\star, 0)$ with $\theta_\star$ the desired position of the hand. Note that the equilibrium on the momentum vector $\mathfrak{p}$ implies $\dot{\theta}_\star = 0$ and $\dot{\varphi}_\star = 0$.

C. Control design

In this paper, we follow the approach proposed in [26] and design the controller for the DoD system via IDA-PBC without solving PDEs in the port-Hamiltonian framework. The main idea in [26] is to design a controller in two steps. First, a partial-feedback linearization as proposed in [30] is performed. This partial-feedback linearisation controller preserves, under certain assumptions, the Hamiltonian structure. This fact has been first shown in [31] and is fundamental for the design in [26]. Second, two passive outputs are identified to build a Lyapunov energy-like candidate function to design a controller that stabilizes the system about an equilibrium point.

We recall here the assumptions made in [26] and [31]. We consider a mechanical system with generic coordinates $\mathbf{q} = (q_a, q_u)$, where q_a and q_u are the actuated and unactuated coordinates, respectively. The mass matrix is written as

$$\mathbf{M}(\mathbf{q}) = \begin{bmatrix} m_{aa} & m_{au} \\ m_{au}^\top & m_{uu} \end{bmatrix}. \tag{17}$$

Then, we make the following assumptions:

A1. The inertia matrix depends only on the unactuated variables q_u, i.e., $\mathbf{M}(\mathbf{q}) = \mathbf{M}(q_u)$.

A2. The sub-block matrix m_{aa} is constant.

A3. The potential energy can be written as $\mathbf{V}(\mathbf{q}) = V_a(q_a) + V_u(q_u)$.

A4. The rows of the matrix $m_{au}(q_u)$ satisfy

$$\frac{\partial (m_{au})_k}{\partial q_{uj}} = \frac{\partial (m_{au})_j}{\partial q_{uk}},\ \forall j \neq k,\ j,k \in \mathcal{I} := \{1, \cdots, n-m\}.$$

The model of the DoD in coordinates (θ, s) used in previous works [5] and [9] does not satisfy the Assumption **A3**, therefore the approach in [26] cannot be applied. However, the change of coordinates $(\theta, s) \to (\theta, \varphi)$ allows transforming the dynamic model such that it satisfies Assumptions **A1**-**A4**. Therefore, we use the dynamics (9) to design the controller.

To design the control law, we first apply a partial-feedback linearisation controller (see [30] for details)

$$\tau_h = \left[M_{11} - \frac{M_{12}^2}{M_{22}}\right] u + \frac{M_{12}}{M_{22}} c_g \sin(\varphi), \tag{18}$$

to obtain a pH system as follows

$$\begin{bmatrix} \dot{q} \\ \dot{p} \end{bmatrix} = \begin{bmatrix} 0 & I_n \\ -I_n & 0 \end{bmatrix} \nabla H(q,p) + \begin{bmatrix} 0 \\ G(q) \end{bmatrix} u \tag{19}$$

where $q = \text{col}(\theta, \varphi)$, $p = \text{col}(p_\theta, p_\varphi) = M(q)\dot{q}$, $G = \text{col}(1, -M_{12})$, and Hamiltonian

$$H = \frac{1}{2} p^\top M^{-1} p + V(q) \tag{20}$$

with $M = \text{diag}(1, M_{22})$. Note that there is a momentum transformation $\mathfrak{p} \to p$ defined as $p = M\mathcal{M}^{-1}\mathfrak{p}$, and a new (acceleration) control input u.

As observed in [26], the partial-feedback linearisation produces, under Assumptions **A1**-**A4**, two passive outputs $y_\theta = p_\theta$ and $y_\varphi = -M_{12}M_{22}^{-1}p_\varphi$. Indeed, considering the storage functions $H_\theta = \frac{1}{2}p_\theta^2$ and $H_\varphi = \frac{1}{2}M_{22}^{-1}p_\varphi^2 + c_g\cos(\varphi)$, we obtain that their time derivatives are

$$\dot{H}_\theta = y_\theta\, u\,, \qquad \dot{H}_\varphi = y_\varphi\, u,$$

which ensure passivity. Note that Assumptions **A1**-**A4** are required to ensure the existence of these two new passive outputs via partial-feedback linearisation.

We propose a desired closed-loop energy function H_d as follows

$$\begin{aligned} H_d &= k_e\left[k_a H_\theta + k_u H_\varphi\right] + \frac{1}{2}K_k\left(k_a y_\theta + k_u y_\varphi\right)^2 \\ &\quad + \frac{1}{2}K_I\left[\int_t (k_a y_\theta + k_u y_\varphi) dt\right]^2. \end{aligned} \tag{21}$$

which is built using the storages energies H_θ and H_φ, a weighted sum of the passive outputs y_θ and y_φ and its integral. The expression (21) can be explicitly written as a state function by substituting H_θ, H_φ, y_θ and y_φ by their expression as functions of the states. After straightforward calculations, we obtain that the desired closed-loop energy can be written as in (3) with desired mass matrix

$$M_d^{-1} = \begin{bmatrix} k_e k_a + k_a^2 K_k & \\ -k_a k_u K_k M_{22}^{-1} M_{12} & -k_a k_u K_k M_{12} M_{22}^{-1} \\ & k_e k_u M_{22}^{-1} + k_u^2 K_k M_{12}^2 M_{22}^{-2} \end{bmatrix} \tag{22}$$

and desired potential function

$$V_d(q) := k_e k_u c_g \cos(\varphi) + \frac{K_I}{2}[k_a\theta - k_u M_{12}(\varphi + c)]^2, \tag{23}$$

with k_e, k_a, k_u, K_k, K_I and c constant parameters to be chosen such that $M_d(q) > 0$, and $q_\star = \arg\min V_d(q)$, and the minimum is isolated.

Proposition 1: Consider the system (19) in closed loop with the control law

$$\begin{aligned} u &= -K^{-1}\left[k_u K_k \frac{M_{12}}{M_{22}} \nabla_\varphi V + K_I[k_a\theta - k_u M_{12}(\varphi + c)]\right] \\ &\quad -K^{-1}K_p\left[k_a p_\theta - k_u \frac{M_{12}}{M_{22}} p_\varphi\right], \end{aligned} \tag{24}$$

with $K = k_e + k_a K_k + k_u K_k \frac{M_{12}^2}{M_{22}}$, and $K_p > 0$. The constants k_e, k_a, k_u, K_k, K_I and c satisfy

$$k_a(k_e + k_a K_k) > 0, \quad k_a k_e k_u K > 0 \tag{25}$$

$$K_I k_a^2 > 0, \quad -k_e k_u > 0 \tag{26}$$

$$K \neq 0, \tag{27}$$

$$c = \frac{k_a}{k_u M_{12}}\theta_\star. \tag{28}$$

Then, the following statements holds

i) The equilibrium $q_{\star 1} = \text{col}(\bar{\theta}, 0)$ of the closed loop, with $K_I = 0$, is asymptotically stable.

ii) The equilibrium $q_{\star 2} = \text{col}(\theta_\star, 0)$ of the closed loop, with $K_I \neq 0$, is asymptotically stable.

Proof First we note that the conditions imposed on the parameters ensure that the desired mass matrix M_d is positive definite, and $q_{1\star}$ and $q_{2\star}$ are minima of the potential energy V_d with $K_I = 0$ and $K_I \neq 0$ respectively. Indeed,

using Sylvester's criterion, the condition of the matrix M_d is satisfied if and only if (25) holds. The minimum conditions on V_d are:
i) $\nabla V_d(q)|_{q=q_\star} = 0 \Leftrightarrow$

$$\left[\begin{array}{c} K_I k_a^2\theta - K_I k_a k_u M_{12}(\varphi + c) \\ -k_e k_u c_g \sin(\varphi) - K_I k_u M_{12}[k_a\theta - k_u M_{12}(\varphi + c)] \end{array}\right]_{q=q_\star} = 0$$

which is satisfied for $q_{\star 1}$ if $K_I = 0$, and for $q_{\star 2}$ with c as in (28).
ii) $\nabla^2 V_d(q)|_{q=q_\star} > 0 \Leftrightarrow$

$$\left[\begin{array}{cc} K_I k_a^2 & -K_I k_a k_u M_{12} \\ -K_I k_a k_u M_{12} & -k_e k_u c_g \cos(\varphi) + K_I k_u^2 M_{12}^2 \end{array}\right]_{q=q_\star} > 0,$$

which is satisfied provided that (26) holds true. The condition (27) ensures that the controller is well-defined.

The stability of the closed loop is shown by choosing H_d as a Lyapunov candidate function. Then, we compute its time derivative along the dynamics (19) as follows

$$\begin{aligned}\dot{H}_d &= (k_a p_\theta - k_u M_{12} M_{22}^{-1} p_\varphi)\Bigg[k_e u + k_a K_k u - k_u K_k \\ &\frac{d}{dt}[-M_{12}M_{22}^{-1}p_\varphi] + K_I[k_a\theta - k_u M_{12}(\varphi + c)]\Bigg] \\ &= \left[k_a p_\theta - k_u \frac{M_{12}}{M_{22}} p_\varphi\right]\left\{\left[k_e + k_a K_k + k_u K_k \frac{M_{12}^2}{M_{22}}\right] u \right. \\ &\left. + \left[k_u K_k \frac{M_{12}}{M_{22}}\nabla_\varphi V + K_I[k_a\theta - k_u M_{12}(\varphi + c)]\right]\right\}.\end{aligned}$$

By using the control law u as proposed in (24), we obtain

$$\dot{H}_d = -K_P\left[k_a p_\theta - k_u \frac{M_{12}}{M_{22}} p_\varphi\right]^2, \tag{29}$$

which ensures stability of the equilibrium. Asymptotic stability follows using the invariance principle and standard Lyapunov theory [32]. Indeed, consider the set $\mathcal{S} = \{(q,p)|\dot{H}_d = 0\}$. Then, we obtain that $k_a M_{22} p_\theta = k_u M_{12} p_\varphi$ holds in $\mathcal{S}$, and by differentiating this equality respect to time, we obtain

$$k_a \dot{p}_\theta = k_u \frac{M_{12}}{M_{22}} \dot{p}_\varphi. \tag{30}$$

The input takes the form $u = \frac{-k_u M_{12} c_g}{M_{22}(k_a + k_u M_{12})}\sin(\varphi)$ from which, by comparing with (24), yields that φ is constant. Therefore $p_\varphi = 0$ and $p_\theta = 0$. Also, the dynamics restricted to $\mathcal{S}$ implies that θ is constant. Moreover, since $\dot{p}_\theta = 0$, then $u = 0$ and $\varphi = 0$, and from (24), we obtain that $\theta = \theta_\star$ when $K_I \neq 0$, otherwise $\theta = \bar{\theta}$. This proves asymptotic stability of the desired equilibrium. □□□

Remark 1: It can be shown that the complexity of the controller τ_h given in (18) with u as in (24) is the same as the one of a controller obtained by using the classical IDA-PBC design, which involves the task of solving the PDEs of the matching equations.

Remark 2: The structure of the proposed controller that asymptotically stabilizes both equilibria $q_{\star 1}$ or $q_{\star 2}$ is the same. The only difference being the gain K_I, which is set to zero to stabilize $q_{\star 1}$, and $K_I \neq 0$ to stabilize $q_{\star 2}$.

D. Closed-loop dynamics

In this section, we show that the closed-loop dynamics of the DoD has the form (4), therefore the control law design in the previous section is an IDA-PBC controller. Notice that the requirement on the closed-loop dynamics was not considered in [26], however here we prove that the closed loop actually preserves the pH form.

Proposition 2: Consider the dynamics of the DoD (9) in closed loop with the controller (18), with u as in (24). Then, the closed-loop dynamics has the pH form (4).

Proof First we note that the partial-feedback control in (18) renders the system in the form (19). Then, we analyse system (19) in closed loop with the inner controller u. The closed loop dynamics has the form (4) if u satisfies

$$-\nabla_q H + G(q)u = -M_d M^{-1}\nabla_q H_d + (J_2 - R)\nabla_p H_d. \tag{31}$$

Using H from (20), H_d from (3) with desired mass matrix and potential function (22) and (23), respectively, and $G = \mathrm{col}(1, -M_{12})$, we obtain

$$-\nabla_q V + Gu = -M_d M^{-1}\nabla_q V_d + (J_2 - R)M_d^{-1} p.$$

We split the control input (24) in $u = u_1 + u_2$ with

$$u_1 = -K^{-1}\left[k_u K_k \frac{M_{12}}{M_{22}}\nabla_\varphi V + K_I[k_a\theta - k_u M_{12}(\varphi + c)]\right] \tag{32}$$

and

$$u_2 = -K^{-1}K_p\left[k_a p_\theta - k_u \frac{M_{12}}{M_{22}} p_\varphi\right]. \tag{33}$$

Then, we will prove that

$$Gu_1 = \nabla_q V - M_d M^{-1}\nabla_q V_d, \tag{34}$$
$$Gu_2 = (J_2 - R)M_d^{-1} p. \tag{35}$$

From (34) we obtain

$$\begin{aligned} M_d^{-1}Gu_1 &= M_d^{-1}\nabla_q V - M^{-1}\nabla_q V_d \\ \left[\begin{array}{c} k_a \\ -k_u\frac{M_{12}}{M_{22}} \end{array}\right] K u_1 &= \left[\begin{array}{c} k_a \\ -k_u\frac{M_{12}}{M_{22}} \end{array}\right]\Bigg[-k_u K_k \frac{M_{12}}{M_{22}}\nabla_\varphi V - \\ &\qquad -K_I[k_a\theta - k_u M_{12}(\varphi + c)]\Bigg], \end{aligned}$$

which is clearly satisfied with u_1 as in (32). From (35) and by setting $J_2 = 0$ and $R = GK^{-1}K_p K^{-1}G^\top$, we obtain

$$\begin{aligned} Gu_2 &= GK^{-1}K_p K^{-1}G^\top M_d^{-1} p \\ Gu_2 &= GK^{-1}K_p\left[\begin{array}{cc} k_a & -k_u\frac{M_{12}}{M_{22}} \end{array}\right] p, \end{aligned}$$

which is satisfied with u_2 as in (33). Therefore, the closed loop has the form (4) as claimed. □□□

Remark 3: Notice that the DoD model used to design the controller does not include damping forces. These forces can compromise the passivity of the closed loop if they are not handle properly. Future research will aim to extend the design approach used here for the case when general damping forces are present in the model.

IV. Simulations

In this section, we present simulations to assess the performance of the controller proposed in Section III-C. We build a simulator of the dynamic model (9) in closed loop with the control law τ_h given in (18). The parameters of the DoD are $r_h = 0.15$ m, $r_o = 0.075$ m, $m_h = 0.335$ Kg, $m_o = 0.220$ Kg and $g = 9.81$ Kgm/s^2, which correspond to the prototype shown in Fig. 2 available at PRISMA Lab and whose detailed description is available in Section V.

The simulations are performed under the following scenario: the DoD starts at rest, and the initial conditions of the balancing and hand angles are $\varphi(0) = 7$ deg and $\theta = 0$ deg, respectively. The desired equilibrium is $q_\star = (0, 0)$, and the controller parameters are $k_a = 0.04$, $k_u = -100$, $k_e = 0.01$, $K_k = 1$, $K_P = 10$ and $K_I = 30$. To enhance the realism to the simulation, we have added noise, a zero-order hold and a time delay of about 0.013 seconds to the measurements. Also, we emulate parameter uncertainties by using different values for the model parameter in the controller and the DoD model (5% deviation). The time histories of the hand and balancing angles are shown in Figs. 3. The plots show that the hand angle converges to the desired set-point, while the object is being balanced on the upright position. Notice that the convergence of the hand angle is slower than the settling time of the balancing angle. There is a small oscillation about the equilibrium due to the measurement noise; however, the control system remains stable. Figure 4 shows the time histories of the balancing and hand angular velocities, as well as the control torque. It can be seen that the trajectories of the velocities are smooth and within acceptable values, and the torque demanded is reasonably smooth and remains bounded by values achievable in a realistic scenario.

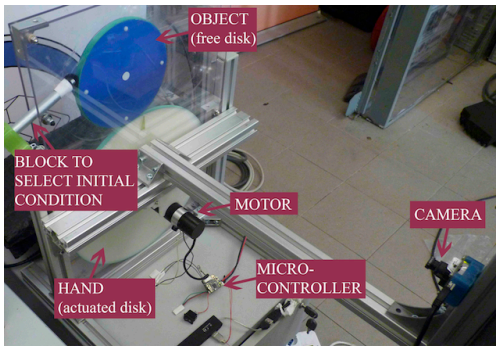

Fig. 2. Prototype of the DoD available at PRISMA Lab.

V. Experiments

A. Experimental set-up

We evaluate the performance of the controller in (18) by using the experimental prototype shown in Fig. 2. The lower disk is actuated by a DC motor (Harmonic Drive RH-8D 3006) equipped with a harmonic drive whose gearhead ratio is 100 : 1, and a 500 p/r quadrature encoder. A rubber band of about 1 mm encircles both disks to avoid slipping. The motor commands are provided by

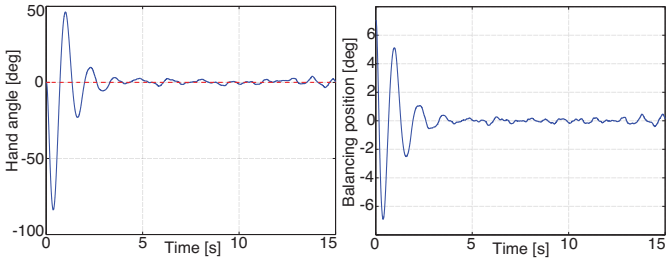

Fig. 3. Time histories of the hand angle $\theta(t)$ (left-hand side) and the balancing angle $\varphi(t)$ (right-hand side). The initial conditions are $\theta(0) = 0$ deg and $\varphi(0) = 7$ deg. The hand reference is $\theta_\star = 0$.

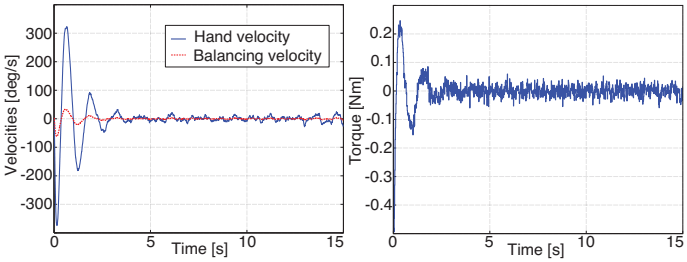

Fig. 4. Time histories of the balancing and hand angular velocities, $\dot{\varphi}(t)$ and $\dot{\theta}(t)$ respectively (left-hand side), and time history of the input torque $\tau_h(t)$ (right-hand side).

an ARM CORTEX M3 microcontroller (32 bit, 75 MHz). This microcontroller receives current references from a PC through an universal serial bus. The microcontroller outputs the current reference for the motor servo, which provides the torque to the hand disk. Therefore, we transform the torque τ_h in (18) in a current control, and we implement an inner-loop current controller written as [5]

$$i_{com} = \frac{\tau_h + \mu_d \dot{\theta} + f_s \mathrm{sgn}(\dot{\theta})}{k_m} + k_p(\hat{\theta} - \theta) + k_d(\dot{\hat{\theta}} - \theta), \quad (36)$$

where $\hat{\theta}$ and $\dot{\hat{\theta}}$ are the desired hand position and velocity, respectively, obtained by integrating (24) at each sample time, while τ_h is given by (18). The parameters k_p and k_d are gains, which were set to 10 and 1, respectively; $k_m = 4.20$ is the motor constant available from the motor datasheet; $\mu_d = 0.29$ is a viscous friction coefficient and $f_s = 0.3$ is the torque required to overcome friction from rest. The values of μ_d and f_s were found by experiments [33]. The inner-loop current controller of the servo motor runs at sample rate of 4KHz. In addition, the microcontroller also provides the measurement of the hand position. The control algorithm, which is written in C++, runs on the external PC with a Linux-based operating system. The position of the object is provided by an external visual system. This visual system consists of an uEye UI-122-xLE camera providing 376×240 pixel images to the PC at 75 Hz, which is also the controller sample rate. In order to speed up computations, a 15×15 pixel region of interest is employed by the image elaboration algorithm running on the same external PC. Notice that the set-up is mounted in full gravity between two plexiglass plates. This differs from [5] and [9], where the gravity is weakened.

B. Case studies

In the first experiment, we set the reference for the hand angle to zero, while the object is desired to be stabilized at the upright position. Under this scenario, we run the experiment using two controllers: the controller proposed in Section III-C, noted as IDA-PBC, and the full-state exact-feedback linearization controller proposed in [5], noted as Linearization. We have tuned the parameters of the controllers at the best of our possibilities. The parameters of the IDA-PBC controller used in the experiments are $k_a = 0.004$, $k_u = -100$, $k_e = 0.01$, $K_k = 1$, $K_P = 5$ and $K_I = 30$; and the parameters of the feedback linearisation controller are $k_1 = 100$, $k_2 = 55$, $k_3 = 117$ and $k_4 = 10$. The left-hand side of Fig. 5 shows that both controllers ensure that the hand converges to the desired position. The plot shows that the IDA-PBC controller drives the hand to the set-point reference faster than the feedback linearization controller, which produces a slow speed of convergence. This advantage is at expense of a larger overshoot on the balance angle. Intuitively, the larger the hand angle motion, the larger the induced balancing angle motion. As can be seen on right-hand side of Fig. 5, both controllers satisfactory balance the object at the upright position. It seems, however, that the closed-loop performance with fast hand convergence and large overshoot or slower hand convergence and small overshoot could be achieved by both controllers if their gain values are appropriately chosen. Figure 6 shows the command torques computed by the IDA-PBC and feedback linearization controllers, and the torques produce by the motor and delivered to the hand. Notice that the inner loop controller produced the necessary torque to compensate the friction forces and unmodeled dynamics of the DC motor. Finally, the normal and frictional forces, computed using (15) and (16) and the experimental data, are shown in Fig. 7. The same figure also display the minimum frictional coefficient $\mu_{min} = \frac{|f_f|}{f_n}$ needed to ensure the rolling assumption. Since the frictional coefficient for the set-up is $\mu > 2$, which is obtained empirically, we infer that the constraints (11) and (12) are satisfied and the rolling assumption is met.

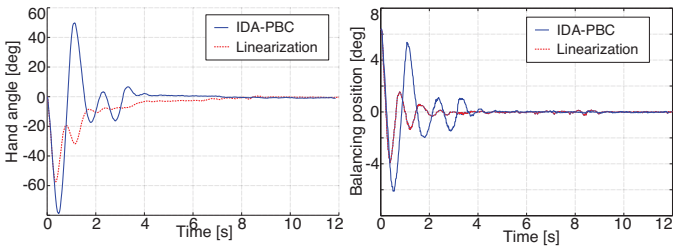

Fig. 5. Time histories of the hand angle $\theta(t)$ (left-hand side) and the balancing angle $\varphi(t)$ (right-hand side). The initial condition is $\theta(0) = 0$ deg and $\varphi(0) = 6.3$ deg, and the hand reference is $\theta_\star = 0$.

In the second experiment, we test the IDA-PBC controller recovering when a non-persistent disturbance acts on the object. The initial conditions are the same as in the first experiment, but now the object is pushed at time about 8 seconds. Figures 8 shows the time history of the hand and balancing angles. Under this scenario, the plots show that the controller recovers the desired equilibrium.

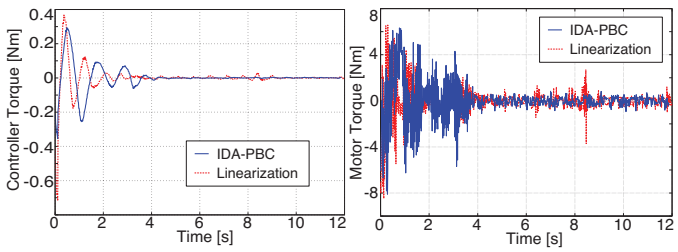

Fig. 6. Time histories of the torque commanded by the controller $\tau_h(t)$ (left-hand side) and the motor torque including compensations $\tau_m(t) = k_m i_{com}(t)$ (right-hand side).

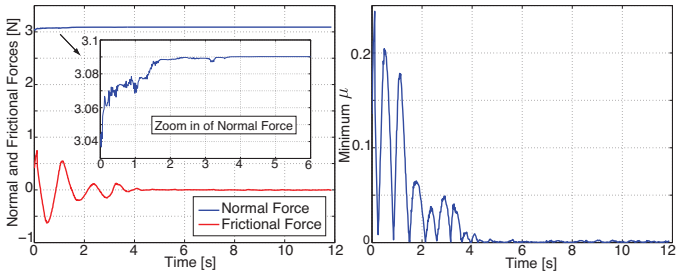

Fig. 7. Time histories of the normal and frictional forces $f_n(t)$ and $f_f(t)$ (left-hand side) and the lower bound for the frictional coefficient $\mu_{min}(t)$ (right-hand side).

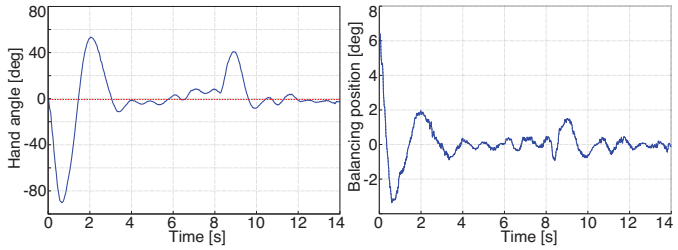

Fig. 8. Time histories of the hand angle $\theta(t)$ (left-hand side) and the balancing angle $\varphi(t)$ (right-hand side). The initial conditions are $\theta(0) = 0$ deg and $\varphi(0) = 6.3$ deg, and the hand reference is $\theta_\star = 0$. A non-persistent disturbance is applied at about $t = 8s$.

In the third experiment, we change the set point of the hand angle, and we set the desired equilibrium to $(\theta_\star, \varphi_\star) = (30°, 0)$. The initial conditions are the same as in the first experiment. The time histories of the hand and balancing angles are depicted in Fig. 9.

The performance of the controller can be visualised in a multimedia video recorded while performing the experiments (available at https://youtu.be/oQ8hS6Hm_e4).

VI. Conclusion and future work

We have investigated an IDA-PBC controller to balance the upright unstable position of the nonprehensile DoD system. We have developed the controller using passivity and pH theory. The controller has been designed without the need of solving PDEs. In addition, we have proved that the closed-loop dynamics retain the pH form. Simulations and experiments bolster the applicability of the

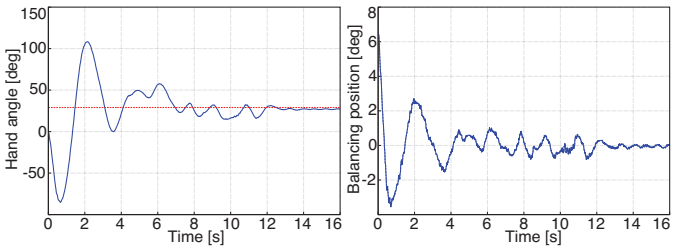

Fig. 9. Time histories of the hand angle $\theta(t)$ (left-hand side) and the balancing angle $\varphi(t)$ (right-hand side). The initial condition is $\theta(0) = 0$ deg and $\varphi(0) = 6.3$ deg, and the hand reference is $\theta_\star = 30°$.

presented theory in practice. In future work, we will focus on the control design of other nonprehensile manipulation primitives and their integration using passivity properties.

Acknowledgment

The research leading to these results has been supported by the RoDyMan project, which has received funding from the European Research Council FP7 Ideas under Advanced Grant agreement number 320992. The authors are solely responsible for the content of this manuscript.

The authors thank A. Fontanelli for his invaluable help in writing the microcontroller code.

References

[1] K. M. Lynch and M. T. Mason, "Dynamic nonprehensile manipulation: Controllability, planning, and experiments," *International Journal of Robotics Research*, vol. 18, no. 1, pp. 64–92, 1999.

[2] M. T. Mason, "Progress in nonprehensile manipulation," *International Journal of Robotics Research*, vol. 18, no. 11, pp. 1129–1141, 1999.

[3] M. Lynch, K and T. D. Murphey, "Control of nonprehensile manipulation," in *Control Problems in Robotics*, A. Bicchi, D. Prattichizzo, and H. Christensen, Eds. Springer Berlin Heidelberg, 2003, pp. 39–57.

[4] K. M. Lynch, N. Shiroma, H. Arai, and K. Tanie, "The roles of shape and motion in dynamic manipulation: The butterfly example," in *IEEE International Conference on Robotics and Automation*, Leuven, Belgium, 1998, pp. 1958–1963.

[5] J.-C. Ryu, F. Ruggiero, and K. M. Lynch, "Control of nonprehensile rolling manipulation: Balancing a disk on a disk," *IEEE Transactions on Robotics*, vol. 29, no. 5, pp. 1152–1161, 2013.

[6] M. Surov, A. Shiriaev, L. Freidovich, S. Gusev, and L. Paramonov, "Case study in non-prehensile manipulation: Planning perpetual rotations for "Butterfly" robot," in *IEEE International Conference on Robotics and Automation*, Seattle, WA, USA, 2015, pp. 1484–1489.

[7] R. Ortega and E. Garcia-Canseco, "Interconnection and damping assignment passivity-based control: A survey," *European Journal of Control*, vol. 10, no. 5, pp. 432–450, 2004.

[8] A. van der Schaft and D. Jeltsema, *Port-Hamiltonian Systems Theory: An Introductory Overview*. The Netherlands: now Publishers Inc, 2014.

[9] J.-C. Ryu, F. Ruggiero, and K. M. Lynch, "Control of nonprehensile rolling manipulation: Balancing a disk on a disk," in *IEEE International Conference on Robotics and Automation*, St. Paul, MN, USA, 2012, pp. 3232–3237.

[10] Z. Li and J. Canny, "Motion of two rigid bodies with rolling constraint," *IEEE Transactions on Robotics and Automation*, vol. 6, no. 1, pp. 62–72, 1990.

[11] S. Awtar, C. Bernard, N. Boklund, A. Master, D. Ueda, and K. Craig, "Mechatronic design of a ball-on-plate balancing system," *Mechatronics*, vol. 12, no. 2, pp. 217–228, 2002.

[12] J. H. Park and Y. J. Lee, "Robust visual servoing for motion control of the ball on a plate," *Mechatronics*, vol. 13, no. 7, pp. 723–738, 2003.

[13] C. Camicia, F. Conticelli, and A. Bicchi, "Nonholonomic kinematics and dynamics of the sphericle," in *IEEE/RSJ International Conference on Intelligent Robots and Systems*, Takamatsu, Japan, 2000, pp. 805–810.

[14] S. Bhattacharya and S. K. Agrawal, "Spherical rolling robot: A design and motion planning studies," *IEEE Transactions on Robotics and Automation*, vol. 16, no. 6, pp. 835–839, 2000.

[15] J. Hauser, S. Sastry, and P. Kokotovic, "Nonlinear control via approximate input-output linearization: The ball and beam example," *IEEE Transactions on Automatic Control*, vol. 37, no. 3, pp. 392–398, 1992.

[16] A. Teel and L. Praly, "Tools for semiglobal stabilization by partial state and output feedback," *SIAM Journal on Control and Optimization*, vol. 33, no. 5, pp. 1443–1488, 1995.

[17] R. Ortega, M. Spong, F. Gomez-Estern, and G. Blankenstein, "Stabilization of a class of underactuated mechanical systems via interconnection and damping assignment," *IEEE Transactions on Automatic Control*, vol. 47, no. 8, pp. 1218–1233, 2002.

[18] C. Barbu, R. J. Sepulchre, W. Lin, and P. V. Kokotovic, "Global asymptotic stabilization of the ball and beam system," in *IEEE Conference on Decision and Control*, San Diego, CA, USA, 1997, pp. 2351–2355.

[19] N. B. Almutairi and M. Zribi, "On the sliding mode control of a ball on a beam system," *Nonlinear Dynamics*, vol. 59, no. 1-2, pp. 221–238, 2010.

[20] D. Hristu-Varsakelis, "The dynamics of a forced sphere plate mechanical system," *IEEE Transactions on Automatic Control*, vol. 46, no. 5, pp. 678–686, 2001.

[21] A. V. Borisov, A. A. Kilin, and I. S. Mamaev, "How to control Chaplygin's sphere using rotors," *Regular and Chaotic Dynamics*, vol. 17, no. 3-4, pp. 258–272, 2012.

[22] M. Cefalo, L. Lanari, and G. Oriolo, "Energy-based control of the butterfly robot," in *8th International IFAC Symposium on Robot Control*, Bologna, Italy, 2006, pp. 1–6.

[23] P. Choudhury and K. M. Lynch, "Rolling manipulation with a single control," *International Journal of Robotics Research*, vol. 21, no. 5-6, pp. 457–487, 2002.

[24] B. Kiss, J. Lévine, and B. Lantos, "On motion planning for robotic manipulation with permanent rolling contacts," *International Journal of Robotics Research*, vol. 21, no. 5-6, pp. 443–461, 2002.

[25] L. Cui and J. S. Dai, "A coordinate-free approach to instantaneous kinematics of two rigid objects with rolling contact and its implications for trajectory planning," in *IEEE International Conference on Robotics and Automation*, Kobe, Japan, 2009, pp. 612–617.

[26] A. Donaire, R. Mehra, R. Ortega, S. Satpute, J. Romero, F. Kazi, and N. Singh, "Shaping the energy of mechanical systems without solving partial differential equations," *IEEE Transactions on Automatic Control*, vol. 61, no. 4, pp. 1051–1056, 2016.

[27] J. Acosta, R. Ortega, A. Astolfi, and A. Mahindrakar, "Interconnection and damping assignment passivity-based control of mechanical systems with underactuation degree one," *IEEE Transactions on Automatic Control*, vol. 50, no. 12, pp. 1936–1955, 2005.

[28] R. M. Murray, Z. Li, and S. S. Sastry, *A mathematical introduction to robotic manipulation*. CRC Press, 1994.

[29] C. L. Saux, R. I. Leine, and C. Glocker, "Dynamics of a rolling disk in the presence of dry friction," *Journal of Nonlinear Sceince*, vol. 15, no. 1, pp. 27–61, 2005.

[30] M. Spong, "Partial feedback linearization of underactuated mechanical systems," in *IEEE/RSJ International Conference on Intelligent Robots and Systems*, Munich, Germany, 1994, pp. 314–321.

[31] I. Sarras, J. Acosta, R. Ortega, and A. Mahindrakar, "Constructive immersion and invariance stabilization for a class of underactuated mechanical systems," *Automatica*, vol. 49, no. 5, pp. 1442–1448, 2013.

[32] H. Khalil, *Nonlinear Systems*. Prentice Hall, 2002.

[33] M. Spong, D. Block, and K. Astrom, "The mechatronics control kit for education and research," in *IEEE Conference on Control Applications*, Mexico City, Mexico, 2001, pp. 105–110.